UNIVERSITY OF
BATH

Link to publication

University of Bath

Structure of plasmonic aerogel and the breakdown of the effective medium approximation

Michael D. W. Grogan,[1] Susannah C. Heck,[2] Katie M. Hood,[1] Stefan A. Maier,[2] and Tim A. Birks[1,*]

[1]*Department of Physics, University of Bath, Bath, BA2 7AY, United Kingdom*

[2]*Department of Physics, Imperial College London, London, SW7 2AZ, United Kingdom*

Corresponding author: t.a.birks@bath.ac.uk

A method for making aerogel doped with gold nanoparticles (GNPs) produces a composite material with a well-defined localized surface plasmon resonance peak at 520 nm. The width of the extinction feature indicates the GNPs are well dispersed in the aerogel, making it suited to optical study. A simple effective medium approximation cannot explain the peak extinction wavelengths. The plasmonic field extends on a scale where aerogel cannot be considered isotropic, so a new model is required: a 5 nm glass coating on the GNPs models the extinction spectrum of the composite material, with air (aerogel), methanol (alcogel), or toluene filling the pores.   © 2011 Optical Society of America

OCIS codes: 160.4670, 250.5403.

Silica aerogel is a highly porous form of glass, with a thin (~5 nm) skeleton encompassing air-filled pores ~50 nm across [1]. It is transparent, but the structure causes Rayleigh-like scattering [2]. The extinction spectrum and photograph, marked (a) in Fig. 1, are typical of regular aerogel.

We developed a method to dope the aerogel with gold nanoparticles (GNPs) during their fabrication, avoiding undesirable aggregation [3,4]. The GNPs cause a reddish color when they are well dispersed in a medium because of a localized dipolar surface plasmon resonance (SPR) [5]. (In contrast aggregated GNPs cause a purple color because they interact with each other, broadening the resonance.) The peak wavelength of the SPR extinction (λ_{SPR}) depends on the size and shape of the GNPs and the refractive properties of the surrounding environment [5]. The extinction spectrum, marked (b) in Fig. 1, shows $\lambda_{SPR} = 520$ nm for the red plasmonic aerogel in photograph (b). Using transmission electron microscopy (TEM) images, we measured the diameter of the predominantly spherical GNPs to be 51 ± 3 nm, although a small number of rods and triangles were observed. The uniform color and TEM images (not shown) of isolated nanoparticles in aerogel indicate that the GNPs are well-distributed randomly throughout the aerogel.

The aerogel was fabricated from base-catalysed 2-step sol-gel chemistry [4]. Tetramethyl orthosilicate, methanol, ammonia, and the aqueous 51 nm GNPs ($\lambda_{SPR} = 535$ nm) were mixed in two steps to form a sol [4], which became a rigid alcogel (a wet-gel with methanol in the pores) 10 min after the second step. We measured $\lambda_{SPR} = 540$ nm in this wet-gel. The aerogel was made by carefully removing the liquid that fills the open network of pores using supercritical drying in CO_2 [4]. Alternatively, the refractive index of the wet-gel can be raised by gradually diffusing toluene into the pores; such a toluene-filled wet-gel had a measured $\lambda_{SPR} = 547$ nm. The concentration of GNPs in the wet-gels was $\approx 10^{12}$ GNPs per cm^3, and none appeared to be lost during supercritical drying.

We used finite element method (FEM) calculations to help understand the structure of plasmonic aerogel. To check our method, we first modeled a GNP in aqueous solution as a spherical 51 nm gold region, surrounded by a region of water (uniform effective index $n_w = 1.33$) extending to a cubic boundary where the extinction cross section σ_{ext} was calculated. The FEM software (Comsol Multiphysics 3.5) has built-in functions for partitioning the simulation space into tetrahedral elements <10 nm. The dielectric constant for the gold region in the simulation used the measured properties reported by Johnson and Christy [6]. The modeled extinction cross section σ_{ext} (m) and experimental extinction (e) spectra in Fig. 2 show good agreement in λ_{SPR}, and the slight broadening in the experimental spectrum is probably caused by the size dispersion of the GNPs. A good agreement was found between the far-field cross sections calculated by FEM and those calculated from Mie theory [7].

To similarly fit our simulations to the 520 and 540 nm peak wavelengths measured for aerogel and alcogel, respectively, we followed the approach of Smith *et al.* [8] who represent the two-component medium around the GNP by a uniform medium with a single effective refractive index. The modeling (solid black curves) matched experiment (red dashed curves) for effective indices of ~1.2 for the aerogel and ~1.4 for the alcogel, as can
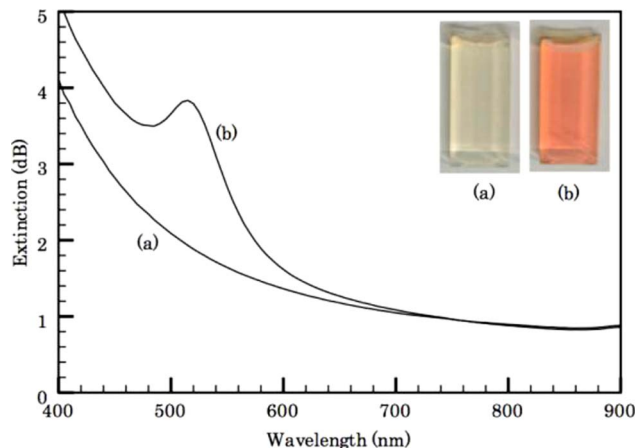

Fig. 1.   (Color online) Extinction spectra and (inset) photographs of (a) undoped aerogel and (b) plasmonic aerogel doped with 50 nm GNPs.
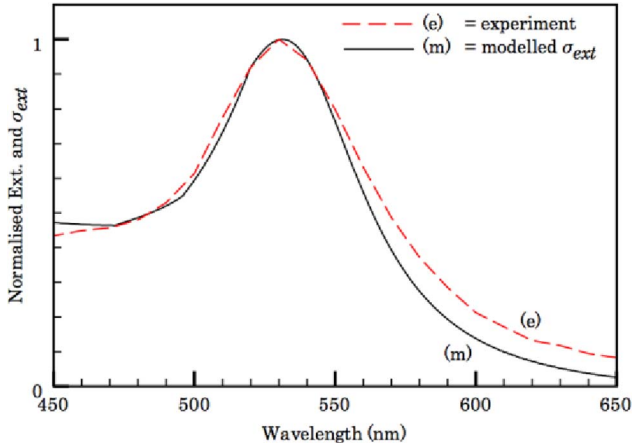
Fig. 2. (Color online) Normalized measured extinction (red dashed curve) and modeled σ_{ext} (solid black curve) of 51 nm GNPs in water.

be seen in Fig. 3(a) curves (1) and (2), respectively. However, this value of 1.2 is very different from the measured aerogel refractive index of 1.05. An effective index of 1.05 gives a peak ~10 nm blueshifted from the one observed, as can be seen when comparing curves (1) and (1a) in Fig. 3(a). We have not measured the index of our alcogel, but it must be close to the 1.33 index of methanol because the alcogels are nearly invisible under methanol. The effective medium value from the fit is therefore different for alcogel as well.

Clearly, a simple effective index model representing the medium around the GNP by any single index does not accurately represent the behavior of GNPs in alcogel or aerogel. This model assumes that the inhomogeneity of the material is much smaller than the wavelength of the light. In aerogel this is generally true, but the wavelength may not be the appropriate length scale once the aerogel is doped with GNPs, due to the confined nature of the electromagnetic field around a metal nanoparticle [9]. This is illustrated by the calculated field around a 51 nm GNP in water, plotted in Fig. 3(b). The field extends only ~50 nm into the host medium, so the SPR is affected only by the material immediately around the GNP rather than the host medium as a whole. Therefore, effective index theories should be used with extreme care where the scale of the medium's internal structure is of the order of the decay length of the SPR.

A model in which the immediate environment of the particle differs from the bulk of the gel seems more appropriate. We considered a 51 nm spherical gold particle with a 5 nm silica coat and embedded in a spatially extensive medium with the refractive index of the appropriate pore fluid (i.e., *not* an effective medium). This "silica-coated" model fits the reported properties of aerogel well in two respects: the solid components of aerogel are silica strands ~5 nm thick [1], and the pores are ~50 nm across [1].

We find good agreement between the σ_{ext} calculated for a silica-coated GNP embedded in a refractive index of 1.00 and the measured extinction spectrum of aerogel, Fig. 4(a) (1). To further test the model, we simulated silica-coated GNPs in refractive index environments of 1.33 and 1.497 for alcogel and toluene wet-gel respectively, Fig. 4(a) curves (2m) and (3m). The corresponding
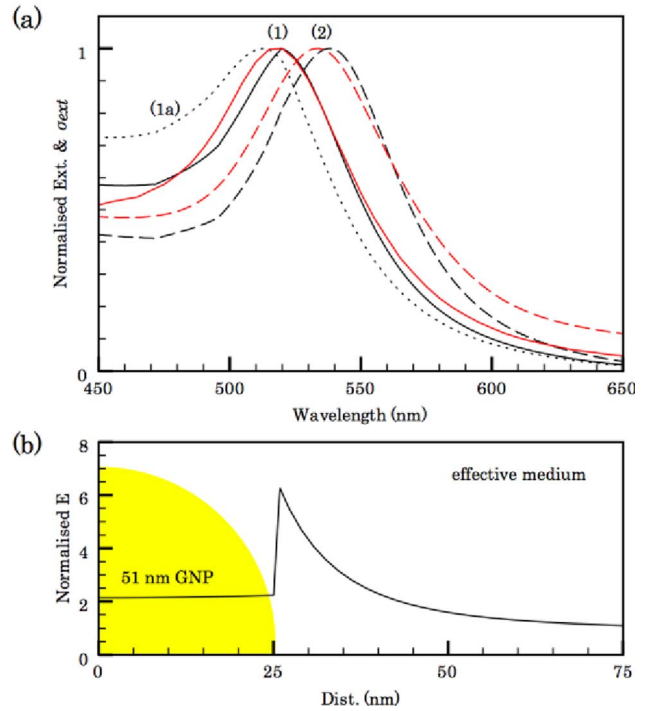

Fig. 3. (Color online) (a) Normalized measured extinction (red curves) and modeled σ_{ext} (black curves) of 51 nm GNPs in aerogel [(1), modeled $n_{\text{eff}} = 1.2$] and alcogel [(2), $n_{\text{eff}} = 1.4$]. (1a) is the modeled σ_{ext} for $n_{\text{eff}} = 1.05$, the measured effective index of the aerogel. (b) Modeled near-field electric field around the GNP, normalized to the incident electric field. The position of the GNP is marked by the shaded area.

experimental curves, Fig. 4(a) curves (2e) and (3e), have λ_{SPR} within 1 nm of the simulation in both cases. We therefore conclude that the silica-coated model accurately reflects the structure of the gel—most likely that the GNPs are wedged in place in the pores and so are effectively surrounded by ~5-nm-thick silica—regardless of the state of the gel.

GNPs have proposed applications in sensing and fluorescence imaging [5,10]. We therefore compared the spatial extent of the electric field for silica-coated and uncoated GNPs and modeled the sensitivity of the SPR wavelength relative to the pore refractive index. Although the 5 nm silica coat might be expected to shield the SPR from its surroundings, we see only a small decrease in the SPR wavelength sensitivity, from ~60 to ~52 nm per unit change of pore refractive index without and with the coat, respectively. This is not unexpected; see Fig. 4(b): the coat does not have a large effect on the SPR decay length in either air or methanol. This indicates that GNP doped aerogel could have sensing applications once optimized using nonspherical and core/shell particles, which have a larger wavelength shift per unit index change [11,12].

The presence of a glass layer around the GNPs would separate them from direct contact with the probe material. This reduces the catalytic potential of the material but is of benefit in surface-enhanced Raman spectroscopy (SERS) [13] as well as enhancing the emission [10,14] from dye and emitter-doped aerogels, which have been proposed for sensor and laser applications [15–17]. It will also help in exploiting nanoparticles of more reactive materials.
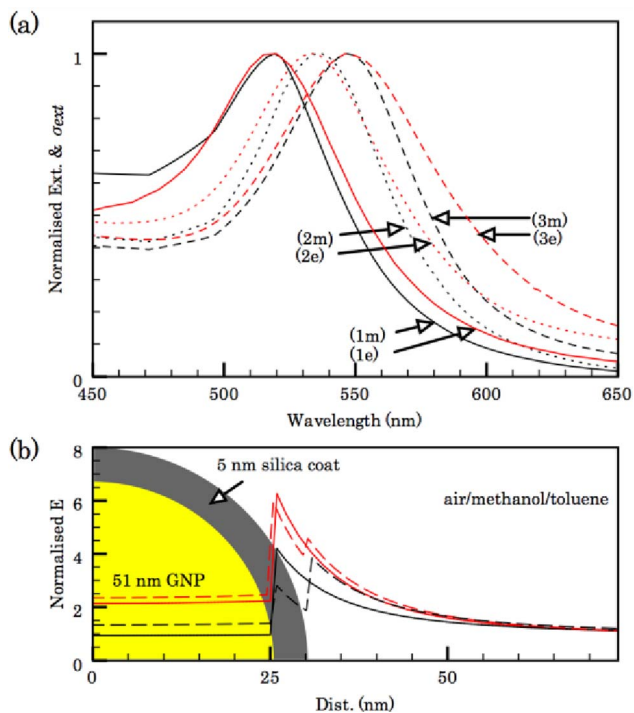
Fig. 4. (Color online) (a) Normalized measured extinction (red lines, marked e) and modeled σ_{ext} (black lines, marked m) of 51 nm GNPs in aerogel (1), alcogel (2), and toluene-filled wet-gel (3). The modeling uses our silica-coated GNP model, with pores filled with the refractive index of air, methanol, and toluene, respectively. The modeled λ_{SPR} is within 1 nm of the experimental data in all cases. (b) Modeled normalized electric field around the silica-coated GNP (dashed curves) compared with an uncoated GNP (solid curves) in air (red curves) and in methanol (black curves). The positions of the GNP and silica coat are marked by the schematic circles.

In conclusion, we have made a plasmonic aerogel by doping with 50 nm GNPs. The pitfalls of simple effective medium approximations for subwavelength structures are highlighted and related to the spatial extent of the SPR field. The location of the GNPs in the aerogel structure has been understood by more accurate modeling of the structure. The particles appear to be completely wedged within the aerogel pores. These plasmonic aerogels are a natural candidate for exploring active plasmonic systems. They offer access to well-separated single GNPs in a thin coat of silica, dispersed in an airlike matrix. The refractive index sensing potential of the material is not greatly diminished as the plasmonic field extends into the aerogel pores. The plasmonic aerogel should have applications in SERS or nonlinear optics [18],

and it may be particularly interesting to co-dope the aerogel to investigate plasmonic gain or lasing.

References

1. J. Fricke and G. Reichenauer, J. Non-Cryst. Solids **95–96**, 1135 (1987).
2. G. M. Pajonk, J. Non-Cryst. Solids **225**, 307 (1998).
3. M. D. W. Grogan, M. D. Rollings, L. M. Xiao, W. J. Wadsworth, R. England, S. A. Maier, and T. A. Birks, in *Conference on Lasers and Electro-Optics* (Optical Society of America, 2010), paper JThE21.
4. M. D. W. Grogan, L. Xiao, T. A. Birks, Department of Physics, University of Bath, Bath, BA2 7AY, UK, R. England, Department of Chemical Engineering, University of Bath, Bath, BA2 7AY, UK, and S. Heck, S. A. Maier, Department of Physics, Imperial College London, London, SW7 2AZ, UK, are preparing a manuscript to be called "Control of nanoparticle aggregation in aerogel hosts."
5. S. A. Maier, *Plasmonics: Fundamentals and Applications* (Springer, 2007).
6. P. B. Johnson and R. W. Christy, Phys. Rev. B **6**, 4370 (1972).
7. M. Born and E. Wolf, *Principles of Optics: Electromagnetic Theory of Propagation, Interference and Diffraction of Light*, 7th ed. (Cambridge University Press, 1999).
8. D. D. Smith, L. A. Snow, L. Sibille, and E. Ignont, J. Non-Cryst. Solids **285**, 256 (2001).
9. W. L. Barnes, J. Opt. A **8**, S87 (2006).
10. M. Pelton, J. Aizpurua, and G. Bryant, Laser Photon. Rev. **2**, 136 (2008).
11. F. Tam, C. Moran, and N. Halas, J. Phys. Chem. B **108** 17290 (2004).
12. C. L. Nehl, H. Liao, and J. H. Hafner, Nano Lett. **6**, 683 (2006).
13. J. F. Li, Y. F. Huang, Y. Ding, Z. L. Yang, S. B. Li, X. S. Zhou, F. R. Fan, W. Zhang, Z. Y. Zhou, D. Y. Wu, B. Ren, Z. L. Wang, and Z. O. Tian, Nature **464**, 392 (2010).
14. K. Aslan, J. R. Lakowicz, H. Szmacinski, and C. D. Geddes, J. Fluoresc. **14**, 677 (2004).
15. N. Leventis, I. A. Elder, D. R. Rolison, M. L. Anderson, and C. I. Merzbacher, Chem. Mater. **11**, 2837 (1999).
16. L. W. Hrubesh, J. Non-Cryst. Solids **225**, 335 (1998).
17. S. Murai, K. Fujita, K. Nakanishi, and K. Hirao, J. Non-Cryst. Solids **345–346**, 438 (2004).
18. R. F. Souza, M. A. R. C. Alencar, E. C. da Silva, M. R. Meneghetti, and J. M. Hickmann, Appl. Phys. Lett. **92**, 201902 (2008).